

Fenton pre-activated grafted modified PVDF membrane and its application in DCMD desalination

Zheng Li*, Jingdong Niu^a, Guangze He^a, Chuntao Zhu, Zicheng Chen, Lanhe Zhang, Jian Zhang, Lin Li and Jian Ming

School of Chemistry Engineering, Northeast Electric Power University, Jilin 132012, Jilin, P. R. China

(Received January 4, 2021, Revised August 17, 2021, Accepted August 17, 2021)

Abstract. As an efficient membrane separation technology, membrane distillation (MD) technology has broad application prospects in desalination of marine and high-salt wastewater. However, membrane fouling/wetting is still the main factor limiting the industrialization of MD technology. In this paper, a polyvinylidene fluoride (PVDF) micro/nano superhydrophobic membrane was prepared using Fenton pretreatment combined with a surface grafting method. Membrane surface hydrophobicity, chemistry and morphology were characterized using measurements of water contact angle (WCA) and liquid entry pressure (LEP), along with observations using attenuated total reflectance-fourier transform infrared spectroscopy (ATR-FTIR), atomic force microscopy (AFM) and scanning electron microscopy (SEM). The grafted fluorinated SiO₂ nanoparticles reduced the surface energy of the PVDF base membrane while at the same time increasing the surface roughness. After modification, the WCA of the PVDF base membrane surface increased from 99° to 155° and the LEP was enhanced from 204 kPa to 235 kPa. Furthermore, the composite membrane revealed stable performance due to the pre-activation by the Fenton solution. The proposed superhydrophobic composite membrane has a great potential to solve the problems of complex membrane pretreatment and prevent damage to the base membrane. The simple method demonstrated here also reduces costs which opens up multiple opportunities for applications in industry.

Keywords: composite membrane; desalination; pre-activated grafting; surface modification; superhydrophobic

1. Introduction

Fresh water resources are facing a crisis of severe shortages due to demand increases, supply reductions and global climate change (Kummu *et al.* 2016, Zhu *et al.* 2018). Desalination is a process of separating dissolved salt from brackish water or salt water to obtain fresh water. It is crucial to alleviate water shortages and ensure the sustainable development of the environment and society in many regions of the world (Panagopoulos and Haralambous 2020, Panagopoulos and Haralambous 2019). Direct contact membrane distillation (DCMD) is the most basic operational method of membrane distillation (MD) technology, and has received extensive attention in heat-driven desalination because of its simple structure and easy realization in industrial applications (Saleh *et al.* 2019, Kiss *et al.* 2018). Membrane material is a core part of the DCMD process as it acts as a barrier between the feed side and the permeate side of the process. Polypropylene (PP), polyvinylidene fluoride (PVDF) and polytetrafluoro-ethylene (PTFE) are good membrane candidates as they provide high-permeate flux due to their high membrane porosity (García Payo *et al.* 2010, Drioli *et al.* 2015, Eykens *et al.* 2017). Among these, PVDF membranes are promising owing to their good hydrophobicity and easy manufacture.

Membrane fouling during the DCMD process can lead to its failure (Mcgaughey *et al.* 2017, Wang and Lin 2017). To date, many methods have been developed to alleviate the problem of membrane fouling in the process of membrane distillation, including pretreatment of the saline water (Kamyar *et al.* 2018, Rezaei *et al.* 2018), optimization of operating conditions (Choi *et al.* 2017, Naidu *et al.* 2014), preparation of new types of membrane with anti-wetting/anti-fouling properties (Liu *et al.* 2020, Xiao *et al.* 2019) and membrane cleaning (Choudhury and Anwar 2019). Of these methods, creating superhydrophobicity membranes by surface modification is proving popular for the development of new anti-wetting and anti-fouling MD membranes (Li *et al.* 2019, Viswanadam *et al.* 2012).

Up to now, the material commonly used to construct superhydrophobic surfaces include silicon dioxide (Lu *et al.* 2016), titanium dioxide (Fan *et al.* 2017), zinc oxide (Zhang *et al.* 2018) and graphene (Li *et al.* 2020). However, nano-silica has unique advantages in constructing superhydrophobic surfaces because of its low cost and the large number of hydroxyl groups in its surface which can facilitate functionalization (Liu *et al.* 2017, Qin *et al.* 2014). There are many methods for constructing superhydrophobic surfaces, such as templating (Zhang *et al.* 2017), surface grafting (Liu *et al.* 2019) and electrospinning and electrodeposition (Liu *et al.* 2015, Ma *et al.* 2018). Nanoarrays have been synthesized using hydrothermal methods (Gao *et al.* 2018, Dong *et al.* 2020). Among these methods, surface grafting which connects the grafted molecular chain to the membrane surface through chemical bonding shows

*Corresponding author, Ph.D., Professor,
E-mail: lizhenghit@126.com

^aM.Eng Student

excellent stability. When PVDF membranes are used, pre-activation is necessary to generate reactive groups on their surface due to their inherent chemical inertia (Tang *et al.* 2017).

Studies have suggested that the pre-activation process can be implemented using ultraviolet light, plasma or high energy radiation (Berthelot *et al.* 2011, Han *et al.* 2016, Liu *et al.* 2006). The ultra violet (UV) irradiation grafting reaction method is mild and the equipment cost is low, but the residual free radicals created on the modified surface may accelerate degradation of the PVDF membrane (Jiménez-Meneses *et al.* 2019). The plasma initiation method needs to be carried out in a vacuum, which limits the application of this method when using large area membranes (Jafari *et al.* 2013). The high-energy rays used in the high-energy radiation method have strong penetration energy, but in the process of irradiation the structure of polymer segments in the membrane being activated can be destroyed and hence its service life can be shortened, limiting its practical application (Liu *et al.* 2006). A further pre-activation method uses the Fenton reaction as this method can oxidize almost all organic compounds (Wang *et al.* 2012). However, recently there has been growing concern about hydroxyl radicals formed by the chain reaction between the divalent iron ion (Fe^{2+}) of the Fenton reagent and hydrogen peroxide. Currently there are few reports describing pre-activation of PVDF membrane using the Fenton reaction followed by preparation of superhydrophobic surfaces using a grafting method.

In this research, we combined surface modification and grafting method to enhance the commercial PVDF membrane surface hydrophobicity. A great deal of hydroxyl groups were generated on the surface of the PVDF base membrane by the Fenton reaction. The PVDF-PFTS/ SiO_2 superhydrophobic membranes were formed by grafting fluorinated modified SiO_2 nanoparticles onto the surface of PVDF-OH membranes. The membranes demonstrated in this paper exhibited great anti-wetting/anti-fouling characteristics and high desalination performance under the direct contact membrane distillation (DCMD) process, which is promising to desalt simulated seawater and oily high-salt wastewater feeds.

2. Materials and methods

2.1 Materials

PVDF flat sheet hydrophobic membranes (0.45 μm) were obtained from Merck Millipore Co., Ltd (Germany). 1H, 1H, 2H, 2H-perfluorooctyl trichlorosilane (PFTS) was obtained from Shang Fu technology Co., Ltd (China). Anhydrous ethanol (99%) and sulfuric acid (98%) was obtained from Beilian Fine Chemicals Co., Ltd (China). Cyclohexane (99%) was obtained from Quanrui Co., Ltd (China). SiO_2 nanoparticles ($\sim 30 \pm 5$ nm), ferrous sulfate ($\text{FeSO}_4 \cdot 7\text{H}_2\text{O}$, AR) and sodium chloride (NaCl, AR) were obtained from Sinopharm Chemical Reagents Co., Ltd (China). Hydrogen peroxide (30%) was obtained from Yongda Chemicals Co., Ltd (China). Vegetable oil was obtained from Jinlongyu Cereals, Oils and Foodstuffs (China). None of the reagents were further purified.

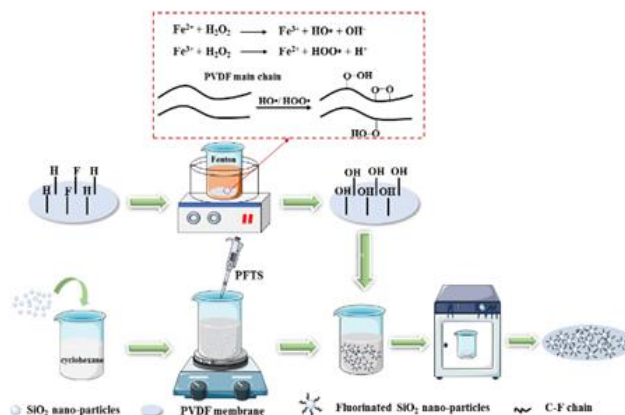


Fig. 1 PVDF-PFTS/ SiO_2 membrane preparation process

2.2 Membrane surface modification

The surface modification process was divided into two steps as shown in Fig. 1.

(1) Pre-activation of the PVDF base membrane surface

The dried PVDF base membrane, 1.39 g of $\text{FeSO}_4 \cdot 7\text{H}_2\text{O}$, 5.5 mL of H_2O_2 and mixed solvent (50 mL ethanol and 50 mL deionized water) were added in a beaker and held in a 50°C water bath for 1 h. The membrane was then cleaned thoroughly using excessive sulfuric acid (98%) and deionized water to remove the adsorbed Fe^{3+} . Finally, PVDF-OH membrane was formed by drying in an oven at 70°C.

(2) Membrane surface grafting

PVDF-PFTS/ SiO_2 superhydrophobic composite membrane was prepared via surface grafting. In the first step, SiO_2 (1.5%) was added to cyclohexane and magnetically stirred for 30 min and then ultrasonically dispersed for 30 min. After the SiO_2 was fully dispersed, PFTS was added dropwise. Ultrasonic dispersion was continued for 30 min at 40°C to obtain a PFTS/ SiO_2 solution. Next, PVDF-OH was impregnated into the prepared PFTS/ SiO_2 solution for 2 h, then the hydrophobic SiO_2 was grafted onto the surface of the PVDF-OH membrane. The grafted PVDF-OH membrane was removed from the PFTS/ SiO_2 solution and dried at 70°C, resulting in a superhydrophobic modified PVDF-PFTS/ SiO_2 membrane.

2.3 Membrane characterization

2.3.1 Contact angle

The change in the hydrophobicity of the membrane surface was measured using a contact angle goniometer (XG-CAM, China). A 3×3 cm² membrane sample was attached to the glass slide of the instrument, and then 5 μL distilled water was dropped onto it. Contact angle measurement instrument matching analysis software was used to calculate the size of the membrane surface water contact angle (WCA).

2.3.2 Surface functional groups

The surface functional groups of the membrane and SiO_2 nanoparticles, obtained during the pre-activation and

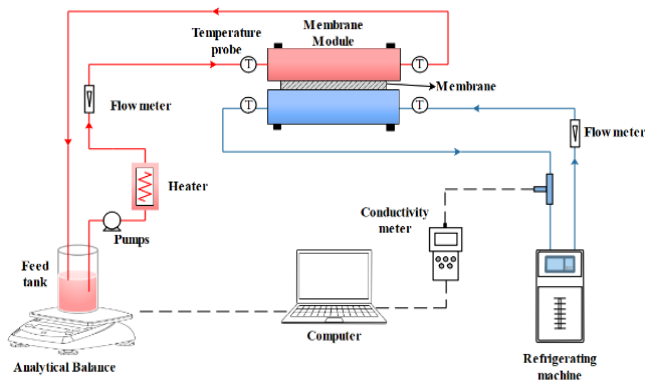


Fig. 2 Self-made direct contact membrane distillation (DCMD) system

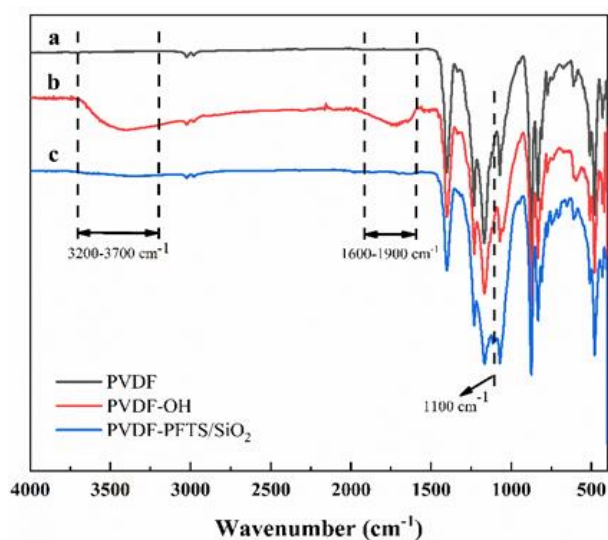


Fig. 3 ATR-FTIR of PVDF base membrane (a), PVDF-OH membrane (b), and PVDF-PFTS/SiO₂ membranes (c)

subsequent grafting, were investigated using an attenuated total reflectance-Fourier transform infrared spectroscope (ATR-FTIR, Nicolet 6700, America). The spectral recording wavenumber was 400 cm⁻¹ to 4000 cm⁻¹.

2.3.3 Surface morphologies and elements

The surface morphologies and rough structure of the membrane were observed using an emission scanning electron microscope (XL30, America) and an atomic force microscope (AFM, Bruker dimension icon, Germany), respectively. The membrane surface average roughness (Ra) was calculated using the matching analysis software of the AFM, and the scanning range was 5 μm × 5 μm. Membrane surface elemental analysis was carried out using energy dispersive X-ray spectroscopy (X-MAX, Britain).

2.3.4 Thermal stability

A thermogravimetric analyzer (TGA, DSC3+, Switzerland) was used to study the membrane thermal stability. Each sample was heated at the rate of 20 °C/min within the temperature range of 35°C to 600°C.

2.3.5 Pore size and liquid entry pressure

A capillary pore size analyzer (Porolux 1000, Germany) was used to obtain the mean and maximum pore size of the prepared membranes. Liquid entry pressure (LEP) was measured using the same capillary pore size analyzer. Nitrogen pressure was increased gradually at the speed of 5 kPa/s, which pushed the water onto the surface of the membrane. The pressure value when water passed through the membrane was defined as the LEP.

2.4 Direct contact membrane distillation system (DCMD)

The performance of the PVDF-PFTS/SiO₂ membranes was evaluated in a simulated DCMD process (Fig. 2). The effective area of the membrane module was 110 cm². The feed solution was simulated seawater (35 g/L NaCl) and oily high-salt wastewater (35 g/L NaCl+ vegetable oil), respectively. The feed solutions were kept to 60°C by an electric heater and circulated at a flow rate of 80 L/h. The water temperature of the permeable solution was controlled by a water cooler at 20°C. The circulation rate was the same as that on the feed side. In the MD process, the conductivity change of the permeate solution was monitored using a conductivity meter (HQ40D, America). The membrane flux was calculated by collecting the changes in the display on the electronic balance (DJ2002FT, China) within a fixed time interval.

3. Results and discussion

3.1 PVDF-PFTS/SiO₂ membrane composition and micro-structure analysis

3.1.1 Surface composition of modified membrane

The infrared spectra obtained from the PVDF base membrane, PVDF-OH membrane and PVDF-PFTS/SiO₂ membrane are shown in Fig. 3. In the ATR-FTIR of the PVDF base membrane (Fig. 3(a)), absorption peaks with wavenumbers at 1071 cm⁻¹, 1170 cm⁻¹ and 3020 cm⁻¹ confirm the existence of the C-F group. The peak at 2980 cm⁻¹ was associated with the C-H stretching vibration, while the peaks at 1401 cm⁻¹ and 835 cm⁻¹ were assigned to the deformation rocking vibration of -CH₂ (Deng *et al.* 2010, Wei *et al.* 2018).

A carbonyl characteristic peak at 1600-1900 cm⁻¹ appeared after the treatment with Fenton solution (Fig. 3(b)), whereas the stretching vibration of -CF₂ at 3020 cm⁻¹ decreased significantly. This suggests that the strong oxidation by the Fenton solution removed the HF from the PVDF chain and formed unsaturated double bonds. The unsaturated double bond then broke and combined with oxygen coming from the solution. In this way hydroxyl groups were formed and this was confirmed by the ATR-FTIR spectra results as a new long and wide absorption band appeared at the characteristic peak of hydroxyl at 3700-3200 cm⁻¹.

The spectra from the membranes grafted with SiO₂ particles (Fig. 3(c)) had almost no hydroxyl characteristic peak compared to the spectra from the PVDF-OH

membrane because of the grafting reaction between the modified SiO₂ nanoparticles and the hydroxyl groups on the surface of PVDF-OH membrane. This indicated that the grafting reaction was successful since the bulk of the hydroxyl groups on the surface of the PVDF-OH membrane were consumed by the modified SiO₂ nanoparticles. In addition, a broad peak which appeared at 1100 cm⁻¹ due to the symmetric stretching vibration of the Si-O-Si bond also confirmed successful grafting (Wang *et al.* 2019).

Fig. 3 also shows that the modified membranes still produced the characteristic peak of the PVDF base membrane, confirming that the process of modification did not change the bulk properties and molecular structure of the PVDF base membrane.

The surface components of the PVDF base membrane, the PVDF-OH membrane, and the PVDF-PFTS/SiO₂ membrane were analyzed using EDS and the results are shown in Fig. 4. The main components of the PVDF base membrane were C and F, with contents of 57.11% and 42.89%, respectively, as PVDF is mainly a resin composed of these two elements. After the Fenton solution treatment, the F on the surface of the membrane decreased, whereas O appeared, which indicated that the strong oxidizing property of the Fenton solution broke the C-F bond to form the -OH group on the surface. The content of O and Si in the PVDF-PFTS/SiO₂ membrane grafted with fluorinated SiO₂ nanoparticles was further increased, which confirmed that the SiO₂ nanoparticles had been grafted to the surface of PVDF-OH membrane.

3.1.2 Surface microstructure of modified membrane

The surface microstructure of a membrane has a significant influence on its hydrophobicity (Ge *et al.* 2014). The SEM images of the PVDF base membrane, the PVDF-OH membrane and the PVDF-PFTS/SiO₂ membrane are shown in Fig. 5. The strong oxidizing property of the Fenton solution resulted in the PVDF base membrane becoming partially carbonized and so the surface of the membrane pre-activated with Fenton solution (Fig. 5(b)) formed a more open high pore structure compared to the PVDF base membrane (Fig. 5(a)). Figs. 5(c1) and 5(c2) show that after PFTS/SiO₂ modification, the PVDF base membrane pores and surface were filled with many fluorinated SiO₂ nanoparticles. Aggregation of fluorinated SiO₂ nanoparticles can also be seen due to the strong interaction between these nanoparticles. These micro/nano binary structures trap a large amount of air, which increases the hydrophobicity of the membrane surface and forms a superhydrophobic surface. Therefore, when water droplets come into contact with the surface of the PVDF-PFTS/SiO₂ membrane, they will immediately roll off, removing contaminants and thereby alleviating membrane fouling and wetting.

AFM was employed to observe the rough structure of roughness (Ra). Three-dimensional morphologies of the PVDF base membrane, the PVDF-OH membrane and the PVDF-PFTS/SiO₂ membrane are shown in Fig. 6. In contrast to the relatively plain surface of the PVDF base membrane (Ra = 217 nm), the average roughness values of the PVDF-OH membrane and PVDF-PFTS/SiO₂ membrane were

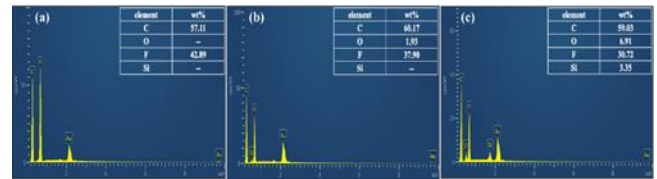


Fig. 4 Chemical composition of PVDF(a), PVDF-OH(b), and PVDF-PFTS/SiO₂(c) membranes surface by EDS analysis

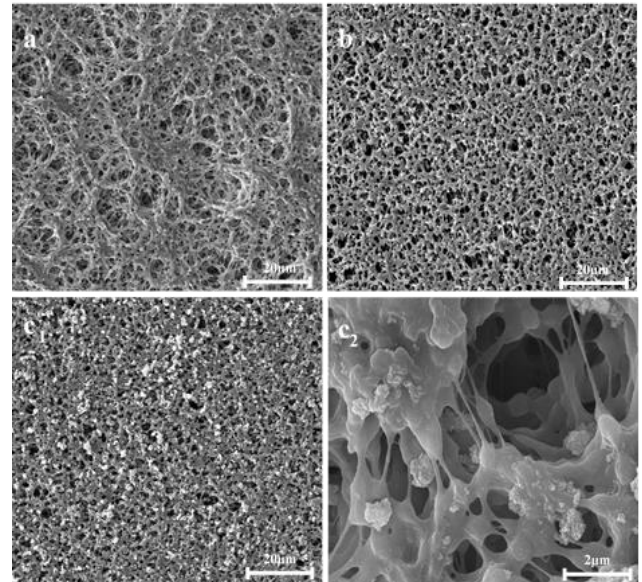


Fig. 5 SEM images of the PVDF base membrane (a), PVDF-OH membrane (b), and PVDF-PFTS/SiO₂ membrane (c1), (c2) High-magnification SEM image of the PVDF-PFTS/SiO₂ membrane (c1)

383 nm and 582 nm, respectively. These results confirmed that a more open porous structure was formed on the surface of the PVDF base membrane after the Fenton solution treatment, and the average roughness increased. The loading of modifying SiO₂ nanoparticles further enhanced the surface roughness to achieve superhydrophobic PVDF membranes. These results are consistent with those from the SEM analysis.

3.1.3 Pore size and LEP of modified membrane

Pore size is the key factor affecting the performance of a porous membrane. The pore sizes of the PVDF base membrane, the PVDF-OH membrane and the PVDF-PFTS/SiO₂ membrane are given in Table 1. The average and largest pore sizes of the PVDF-OH membrane modified by the Fenton solution were larger than those of the PVDF base membrane, with a maximum pore size of 690 nm and an average pore size of 570 nm. This confirmed that a more open pore structure in the PVDF membrane was obtained following the strong oxidation of the Fenton solution. After further grafting of PFTS/SiO₂, the maximum and average pore size of the PVDF-OH membrane decreased to 664 nm and 561 nm, respectively. This was because of the aggregation of fluorinated SiO₂ nanoparticles on the surface and pores of the PVDF-OH membrane. In addition, it can

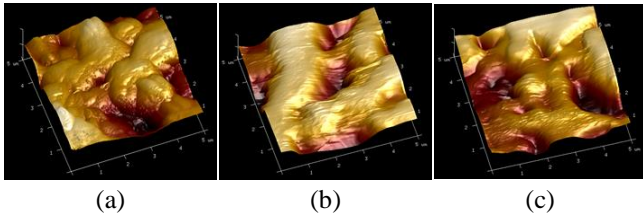


Fig. 6 AFM image of the three-dimensional morphology of PVDF base membrane (a), PVDF-OH membrane (b) and PVDF-PFTS/SiO₂ membrane (c)

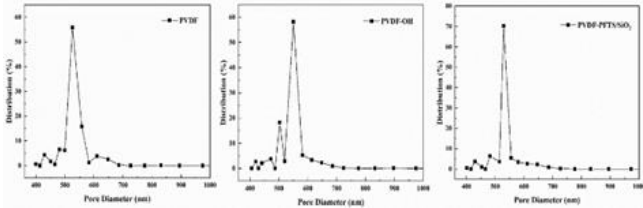


Fig. 7 Pore size distributions of PVDF base membrane, PVDF-OH membrane and PVDF-PFTS/SiO₂ membrane

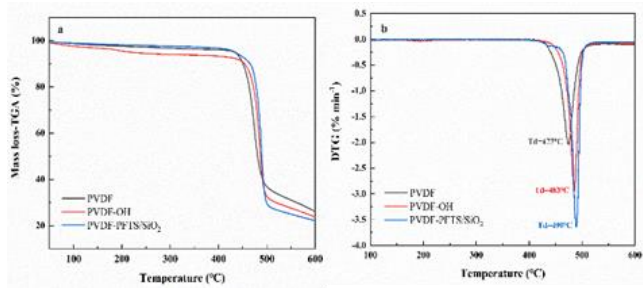


Fig. 8 Thermo gravimetric analysis (TGA) (a) and Derivative thermo gravimetric (DTG) analysis (b) of PVDF base membrane, PVDF-OH membrane and PVDF-PFTS/SiO₂ membrane

be seen from Fig. 7 that the addition of SiO₂ nanoparticles makes the pore size distribution of the PVDF base membrane narrower and more uniform.

The LEP is an important index of membrane wettability. When the pressure on the hot side of a membrane is higher than the LEP of the membrane itself, pore wetting will occur and lead to fouling by the permeable liquid and a decrease of the membrane flux (El-Bourawi *et al.* 2006). The Laplace equation states that the LEP value is not only related to the structure of the membrane itself, but also related to its surface properties (Franken *et al.* 1987). The specific relationship is:

$$P_{liquid}P_{vapor} = \frac{-2\gamma B \cos \theta}{r_{max}} < LEP. \quad (1)$$

where B indicates the geometric factor which is a parameter related to the membrane structure, γ is the surface tension of the droplet, θ is the contact angle of the liquid and r_{max} is the maximum pore size of the membrane.

Owing to the decrease in hydrophobicity and the increase in the largest pore size of the PVDF-OH membrane, LEP decreased from 204 kPa for the base membrane to 195 kPa for the PVDF-OH membrane.

Although the maximum pore size of the PVDF base membrane was slightly smaller than that of the PVDF-PFTS/SiO₂ membrane, the PVDF-PFTS/SiO₂ membrane was much more hydrophobic than the PVDF base membrane, resulting in an increase in the membrane LEP from 204 kPa to 235 kPa.

Silica nanoparticles can act as a crosslinking point in composite membranes, which can increase the rigidity of polymeric chains and result in improved membrane mechanical performance (Lai *et al.* 2014). The tensile strength was increased from 39.8 MPa for the PVDF base membrane to 43.6 MPa after modification with fluorinated SiO₂ nanoparticles. However, the addition of fluorinated SiO₂ nanoparticles increased the brittleness of the PVDF base membrane, and the tensile strain at the fracture was reduced from 19% to 17%.

3.2 PVDF-PFTS/SiO₂ membrane stability analysis

3.2.1 Thermal stability of the PVDF-PFTS/SiO₂ membrane

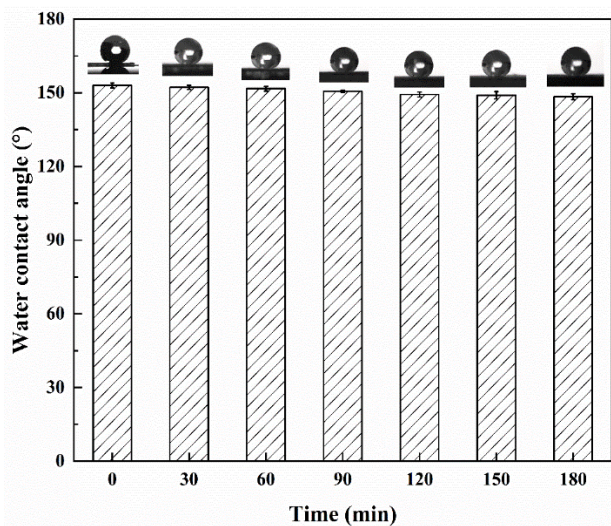
One of the main requirements of a hydrophobic membrane is high thermal stability. Therefore, TGA tests were conducted to analyze the difference in thermal stability between the PVDF base membrane and the modified membranes. The results showed that all samples had nearly the same thermal trend with good thermal stability (Fig. 8). The PVDF base membrane, the PVDF-OH membrane, and the PVDF-PFTS/SiO₂ membrane first showed decomposition at 473°C, 483°C and 490°C, respectively. Contrasted with the PVDF base membrane, the decomposition temperatures of the PVDF-OH membrane and the PVDF-PFTS/SiO₂ membrane increased by 10°C and 17°C, respectively. The thermal stability of the PVDF-OH membrane was better than that of the PVDF base membrane, and the thermal stability improved further after PFTS/SiO₂ grafting. SiO₂ particles have strong thermal stability with a heat-insulating effect during the heating process, which may explain the delay in the decomposition of the PVDF-PFTS/SiO₂ membrane. In addition, the hydroxyl groups on the surface of fluorinated SiO₂ can form hydrogen bonds with the surface of the pre-activated PVDF membrane. These hydrogen bonds are able to limit the thermal movement of the PVDF macromolecular chain and increase energy needed for the movement and fracture of the PVDF-PFTS/SiO₂ membrane macromolecular chain (Gaur *et al.* 2015, Yu *et al.* 2009). The weight of all samples decreased by about 65% at 500°C, and this decrease continued with increasing temperature, because of the decomposition of the PVDF polymer backbone.

3.2.2 Durability of the PVDF-PFTS/SiO₂ membrane

The PVDF-PFTS/SiO₂ membrane was treated in an ultrasonic cleaner at 75°C for 3 h, and its durability was assessed by detecting any change in its surface hydrophobicity. Change in surface hydrophobicity was observed by measuring the WCA every 30 min (Fig. 9). After 3 h of sonication, the surface hydrophobicity of the PVDF-PFTS/SiO₂ membrane showed a slight decrease, but still had a long-lasting stable high hydrophobic surface with

Table 1 Parameter of PVDF base membrane, PVDF-OH membrane and PVDF-PFTS/SiO₂ membrane

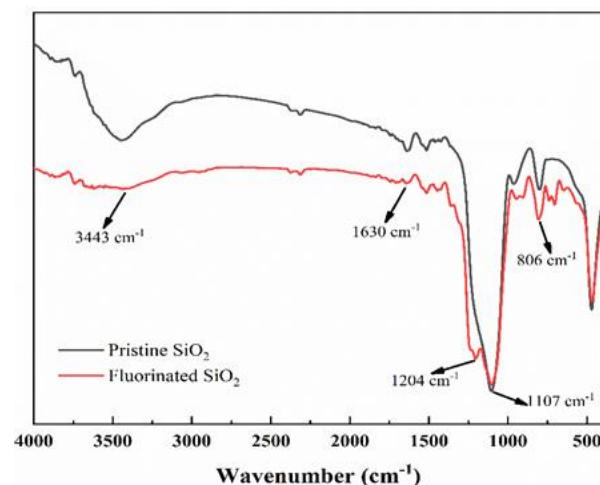
Sample	Membrane thickness (μm)	Max pore size (nm)	Mean pore size (nm)	WCA ($^{\circ}$)	LEPw (kPa)	Tensile strength (MPa)	Tensile stain at break (%)
PVDF	100 \pm 1	652	543	100 \pm 1	204	39.8	19
PVDF-OH	99 \pm 1	690	570	85 \pm 1	195	35.2	25
PVDF-PFTS/SiO ₂	101 \pm 1	664	561	153 \pm 2	235	43.6	17

Fig. 9 The change of water contact angle of PVDF-PFTS/SiO₂ membrane surface with ultrasonic time

a WCA of 149.6°. The results indicate that the superhydrophobic surface formed by grafting fluorinated SiO₂ nanoparticles on to the surface of PVDF base membrane treated with Fenton solution has good stability and durability, and has broad application prospects in membrane distillation technology.

3.3 Superhydrophobic mechanisms of the PVDF-PFTS/SiO₂ membrane

The hydrophobicity of a solid surface lies in its low surface energy and surface structure with multi-stage roughness (Wang *et al.* 2008). It is well-known that 1H, 1H, 2H, 2H-perfluorooctyltrichlorosilane (PFTS) has an extremely low surface energy because of its high content of -CF₃ (6.7 mN/m) and -CF₂ (16 mN/m) groups (Meng *et al.* 2008, Saifaldeen *et al.* 2016). The surface energy can be further reduced, and its wettability can be adjusted, after the solid surface is treated with appropriate molecules. In this study, SiO₂ nanoparticles were fluorinated and then grafted onto the surface of PVDF base membrane using 1H, 1H, 2H, 2H-perfluorooctyl trichlorosilane (PFTS). The specific reaction process can be divided into two parts. Firstly, In the presence of water, the hydrophilic trichlorosilane head of the PFTS molecule is hydrolyzed to generate trisilanol. The hydroxyl groups on the head of the trisilanol and part of the hydroxyl groups on the surface of the SiO₂ form a bond of Si-O-Si to fix the PFTS molecules onto the surface of the SiO₂ nanoparticles. Next, the remaining hydroxyl groups on the surface of the fluorinated SiO₂ combine with the hydroxyl radicals generated on the surface of the PVDF

Fig. 10 FTIR spectra of pristine and fluorinated SiO₂ nanoparticles

base membrane treated with the Fenton solution, and the fluorinated SiO₂ nanoparticles are grafted onto the surface of the PVDF membrane. Therefore, fluorination modification of SiO₂ is a key step in the preparation of composite membranes.

To prove the modification results, the chemical composition of the fluorinated SiO₂ nanoparticles and pristine SiO₂ were characterized using ATR-FTIR spectrometry (Fig. 10). Spectral peaks at 1107 cm⁻¹ and 806 cm⁻¹ were characteristic of Si-O-Si stretching vibration and bending vibration in SiO₂, respectively (Lin *et al.* 2014). The characteristic peak generated by the symmetric stretching vibration of -OH was about 3440 cm⁻¹, while the absorption peak at 1630 cm⁻¹ was derived from the bending vibration of -OH in the physical adsorption water (Abdolmaleki *et al.* 2011, Vejayakumaran and Rahman 2008). These characteristic peaks indicated that the modification reaction did not change the main structure of SiO₂. The peak of the C-F bond appeared at 1204 cm⁻¹ in the fluoroalkyl chlorosilane after the modification reaction (Gao *et al.* 2006), while the -OH characteristic peak at 3443 cm⁻¹ was also significantly weakened. These results indicate that the fluoroalkyl groups were successfully grafted onto the surface of the SiO₂ nanoparticles after the modification. The water contact angle of the virgin and fluorinated SiO₂ nanoparticles were measured and results are presented in Fig. 11. The WCA of the fluorinated SiO₂ nanoparticles increased from 0° to 146°. This also confirms that the SiO₂ nanoparticles had good hydrophobicity after fluorination modification.

The measured WCA values can be used in the Cassie-Baxter model in order to explain the reason for the change

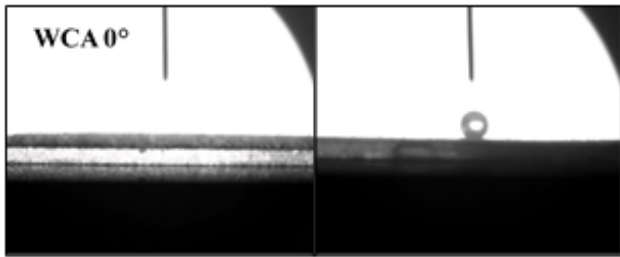


Fig. 11 Water contact angle (WCA) of the virgin (left) and fluorinated SiO₂ nanoparticles (right)

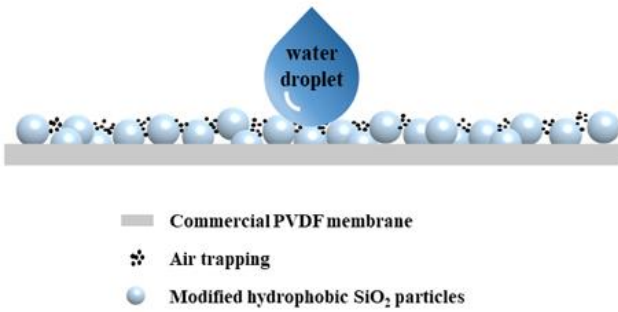


Fig. 12 Schematic diagrams of modified superhydrophobic membrane surface

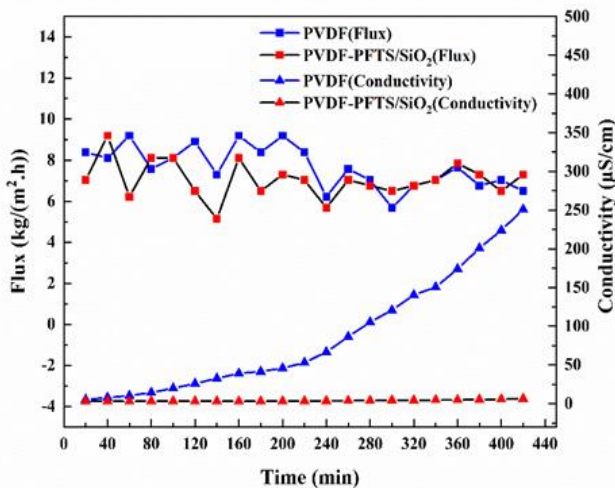


Fig. 13 Membrane flux and permeate conductivity for PVDF base membrane and PVDF-PFTS/SiO₂ membranes in DCMD via feeding NaCl solution (3.5 wt%)



Fig. 14 Surface state of PVDF base membrane (a) and PVDF-PFTS/SiO₂ membrane (b) after DCMD experiment NaCl solution (3.5 wt%) was used as the feed solution

in hydrophobicity of the modified membrane surface (Nosonovsky and Michael 2007). According to Cassie-Baxter theory, the interface between droplet and rough surface is a composite interface consisting of liquid/solid and liquid/gas interfaces. Since the droplet size is larger than the size of the microstructure of the rough surface, the droplet cannot penetrate into the groove of the rough surface, and so air is trapped between the droplets and the rough surface. The Cassie equation (Cassie 1948) is as follows:

$$\cos \theta_n = f_1 \cos \theta_1 + f_2 \cos \theta_2 \quad (2)$$

$$f_1 + f_2 = 1 \quad (3)$$

Here, θ_n is the apparent contact angle of the modified membrane, f_1 and f_2 are the ratio of liquid/solid to liquid/gas contact area to total contact area, respectively. θ_1 and θ_2 are the eigen contact angle of the liquid/solid and liquid/gas interfaces, respectively, and $\theta_2 = 180^\circ$. Eq. (2) can be transformed into:

$$\cos \theta_n = f_1 \cos \theta_1 + f_1 - 1 \quad (4)$$

The water contact angle of a smooth surface PVDF base membrane can only reach as high as 98° (i.e., $\theta_1 = 98^\circ$) while the contact angle of the PVDF-PFTS/SiO₂ membrane was 152° ($\theta_n = 152^\circ$), and f was calculated to be 0.139. This meant that when the droplets were placed on the prepared superhydrophobic PVDF-PFTS/SiO₂ membrane surface, only 13.9% of the PVDF-PFTS/SiO₂ membrane surface came into contact with the droplets. Therefore, it can be confirmed that a micro/nano multi-level rough surface was constructed after fluorinated SiO₂ nanoparticles were grafted onto the surface of the PVDF-OH membrane. The surface can be regarded as a rough, porous structure. As the amount of air between water droplets and the membrane surface increased, the contact area between the droplets and the membrane surface decreased. Thus, the hydrophobicity of the modified membrane surface was increased, and a superhydrophobic surface was obtained (Fig. 12).

3.4 PVDF-PFTS/SiO₂ membrane performances during the DCMD process

A DCMD simulation was carried out using 3.5 wt% NaCl as the feed solution. The electrical conductivity of the permeate and the membrane flux were compared between the PVDF base membrane and PVDF-PFTS/SiO₂ membranes (Fig. 13). The permeation flux of the PVDF base membrane was approximately 7.7 kg/m²h which was slightly higher than that of the superhydrophobic PVDF-PFTS/SiO₂ membrane (7.0 kg/m²h). The main reason for the decrease of permeation flux of the PVDF-PFTS/SiO₂ membrane was that a fluorinated SiO₂ layer formed on the membrane surface after surface grafting, which increased the membrane thickness and slowed down the mass transfer slightly. In addition, the PVDF base membrane showed stable permeation flux for 4 h before operation. After 7 h of operation, the permeation flux gradually decreased to about

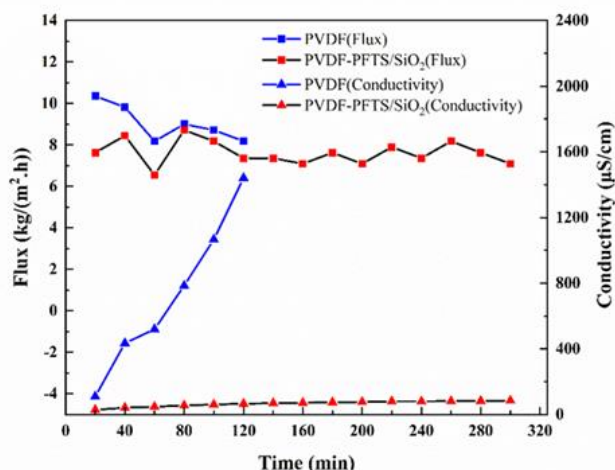


Fig. 15 Membrane flux and permeate conductivity for PVDF base membrane and PVDF-PFTS/SiO₂ membranes in DCMD via feeding simulated oily high-salt wastewater



Fig. 16 Simulated oily high-salt wastewater was used as the feed solution, the surface state of PVDF base membrane(a) and PVDF-PFTS/SiO₂ membrane(b) after DCMD experiment

77% of the original flux, and the permeation conductivity gradually increased to 256 $\mu\text{S}/\text{cm}$. Obvious wetting was observed on the surface of the PVDF base membrane after the DCMD simulation (Fig. 14).

The PVDF-PFTS/SiO₂ membrane was quite stable during its entire operation and permeation flux and conductivity of the PVDF-PFTS/SiO₂ membrane did not change significantly. The main reason for this result was that the PVDF base membrane was more likely to be wetted and fouled than the PVDF-PFTS/SiO₂ membrane. Owing to the grafting of fluorinated SiO₂ particles, the PVDF-PFTS/SiO₂ membrane had very low surface energy and high surface roughness. The inorganic salts in the feed solution were not easily accumulated or adsorbed onto the PVDF-PFTS/SiO₂ membrane surface. Hence, the pores of the PVDF-PFTS/SiO₂ membrane were not easily wetted and fouled, and hence had better stability and durability than the PVDF base membrane.

The DCMD simulation was also carried out using oily high-salt wastewater as the feed solution, and the anti-fouling/anti-wetting properties of the PVDF base membrane and the PVDF-PFTS/SiO₂ membrane were compared. The electrical conductivity of the PVDF base membrane increased sharply and the flux decreased slowly within 2 hours of operation, which indicated that the membrane had been partially wetted, resulting in

high-concentration NaCl being transferred directly through the membrane to the permeate side (Fig. 15). Compared with the PVDF base membrane, the superhydrophobic PVDF-PFTS/SiO₂ membrane had better anti-wetting/anti-fouling performance, and the desalination rate was maintained at 99.85%. The combination of multiple levels of roughness structures and low surface energy made it difficult for the surface of the PVDF-PFTS/SiO₂ membrane to contact the feed solution, reducing the adsorption of oil contaminant onto the surface of the membrane, thus preventing the superhydrophobicity membrane from being wetted.

By observing the surface state of the membranes after the DCMD simulation, it can be clearly seen that the surface of the PVDF base membrane was obviously wetted by the adsorption of oil, while the surface of the superhydrophobic membrane was still very clean with only slight wetting (Fig. 16). Therefore, the PVDF-PFTS/SiO₂ membrane demonstrated stable anti-wetting/anti-fouling properties. Hence the superhydrophobic PVDF-PFTS/SiO₂ membrane prepared by this method is a good choice for extracting water from high saline feed solution containing hydrophobic pollutants using the membrane distillation process.

4. Conclusions

In this paper a new membrane modification method is developed, with the pretreatment of PVDF base membrane by Fenton solution, followed by grafting of hydrophobic fluorinated SiO₂ nanoparticles, providing a technically feasible and economically reasonable choice for the preparation of stable and durable of superhydrophobic composite membranes.

- The results indicated that after grafting with fluorinated SiO₂ nanoparticles, the surface energy of PVDF base membrane is decreased and the surface roughness is increased (from 217 nm to 582 nm), resulting in the water contact angle of the PVDF increasing from 99° to 155°.

- In addition, the grafting of SiO₂ nanoparticles made the pore size distribution of the PVDF membrane narrower and more uniform.

- Pre-activation of the PVDF membrane using Fenton solution made the fluorinated SiO₂ layer more stable and producing good anti-fouling/anti-wetting ability during membrane distillation desalination.

- Therefore, this method is expected to provide a new approach and inspire new ideas for industrial applications of superhydrophobic surface preparation and membrane distillation desalination technologies.

Acknowledgments

This work was supported by the Jilin Province Science and Technology Development Project of China [20180101309 JC].

References

Abdolmaleki, A., Mallakpour, S. and Borandeh, S. (2011),

- “Preparation, characterization and surface morphology of novel optically active poly(ester-amide)/functionalized ZnO bionanocomposites via ultrasonication assisted process”, *Appl. Surf. Sci.*, **257**(15), 6725-6733.
<https://doi.org/10.1016/j.apsusc.2011.02.112>.
- Berthelot, T., Le, X.T., Jégou, P., Viel, P., Boizot, B., Baudin, C. and Palacin, S. (2011), “Photoactivated surface grafting from PVDF surfaces”, *Appl. Surf. Sci.*, **257**(22), 9473-9479.
<https://doi.org/10.1016/j.apsusc.2011.06.039>.
- Cassie, A.B.D. (1948), “Contact angles”, *Discuss. Faraday. Soc.*, **3**(5), 11-16. <https://doi.org/10.1039/DF9480300011>.
- Choi, J., Choi, Y., Jang, Y., Shin, Y. and Lee, S. (2017), “Effect of aeration on CaSO₄ scaling in membrane distillation process”, *Desalin. Water Treat.*, **90**, 7-15.
<https://doi.org/10.5004/dwt.2017.21349>.
- Choudhury, M.R., Anwar, N., Jassby, D. and Rahaman, M.S. (2019), “Fouling and wetting in the membrane distillation driven wastewater reclamation process—A review”, *Adv. Colloid Interf. Sci.*, **269**(1), 370-399.
<https://doi.org/10.1016/j.cis.2019.04.008>.
- Deng, B.O., Ming, Y.U., Yang, X., Zhang, B., Linfan, L.I., Xie, L., Jingye, L.I. and Xiaofeng, L.U. (2010), “Antifouling microfiltration membranes prepared from acrylic acid or methacrylic acid grafted poly (vinylidene fluoride) powder synthesized via pre-irradiation induced graft polymerization”, *J. Membr. Sci.*, **350**(1), 252-258.
<https://doi.org/10.1016/j.memsci.2009.12.035>.
- Dong, S., Yun, Y., Wang, M., Li, C., Fu, H., Li, X., Yang, W. and Liu, G. (2020), “Superhydrophobic alumina hollow ceramic membrane modified by TiO₂ nanorod array for vacuum membrane distillation”, *J. Taiwan Inst. Chem. E.*, **117**, 56-62.
<https://doi.org/10.1016/j.jtice.2020.11.030>.
- Drioli, E., Ali, A. and Macedonio, F. (2015), “Membrane distillation: Recent developments and perspectives”, *Desalination*, **356**, 56-84.
<https://doi.org/10.1016/j.desal.2014.10.028>.
- El-Bourawi, M.S., Ding, Z., Ma, R. and Khayet, M. (2006), “A framework for better understanding membrane distillation separation process”, *J. Membr. Sci.*, **285**(1), 4-29.
<https://doi.org/10.1016/j.memsci.2006.08.002>.
- Eykens, L., De Sitter, K., Dotremont, C., Pinoy, L. and Van der Bruggen, B. (2017), “Membrane synthesis for membrane distillation: A review”, *Sep. Purif. Technol.*, **182**, 36-51.
<https://doi.org/10.1016/j.seppur.2017.03.035>.
- Fan, Y., Chen, S., Zhao, H. and Liu, Y. (2017), “Distillation membrane constructed by TiO₂ nanofiber followed by fluorination for excellent water desalination performance”, *Desalination*, **405**, 51-58.
<https://doi.org/10.1016/j.desal.2016.11.028>.
- Franken, A.C.M., Nolten, J.A.M., Mulder, M.H.V., Bargeman, D. and Smolders, C.A. (1987), “Wetting criteria for the applicability of membrane distillation”, *J. Membr. Sci.*, **33**(3), 315-328. [https://doi.org/10.1016/S0376-7388\(00\)80288-4](https://doi.org/10.1016/S0376-7388(00)80288-4).
- Gao, J., Wang, X., Wei, Y. and Yang, W. (2006), “Synthesis and characterization of a novel fluorine-containing polymer emulsion with core/shell structure”, *J. Fluorine. Chem.*, **127**(2), 282-286. <https://doi.org/10.1016/j.jfluchem.2005.12.002>.
- Gao, X., Wen, G. and Guo, Z. (2018), “Durable superhydrophobic and underwater superoleophobic cotton fabrics growing zinc oxide nanoarrays for application in separation of heavy/light oil and water mixtures as need”, *Colloid Surface A*, **559**, 115-126.
<https://doi.org/10.1016/j.colsurfa.2018.09.041>.
- García Payo, M.D.C., Essalhi, M., Khayet Souhaimi, M., García Fernández, L., Charfi, K. and Arafat, H. (2010), “Water desalination by membrane distillation using PVDF-HFP hollow fiber membranes”, *Membr. Water Treat.*, **1**(3), 215-230.
<https://doi.org/10.12989/mwt.2010.1.3.215>.
- Gaur, M.S., Indolia, A.P., Rogachev, A.A. and Rahachou, A.V. (2015), “Influence of SiO₂ nanoparticles on morphological, thermal, and dielectric properties of PVDF”, *J. Therm. Anal. Calorim.*, **122**(3), 1403-1416.
<https://doi.org/10.1007/s10973-015-4872-x>.
- Ge, B., Zhang, Z., Men, X., Zhu, X. and Zhou, X. (2014), “Sprayed superamphiphobic coatings on copper substrate with enhanced corrosive resistance”, *Appl. Surf. Sci.*, **293**, 271-274.
<https://doi.org/10.1016/j.apsusc.2013.12.148>.
- Han, Y., Song, S., Lu, Y., Zhu, D. (2016), “A method to modify PVDF microfiltration membrane via ATRP with low-temperature plasma pretreatment”, *Appl. Surf. Sci.*, **379**, 474-479. <https://doi.org/10.1016/j.apsusc.2016.04.114>.
- Jafari, R., Asadollahi, S. and Farzaneh, M. (2013), “Applications of plasma technology in development of superhydrophobic surfaces”, *Plasma Chem. Plasma P.*, **33**(1), 177-200.
<https://doi.org/10.1007/s11090-012-9413-9>.
- Jiménez-Meneses, P., Bañuls, M., Puchades, R. and Maquieira, Á. (2019), “Novel and rapid activation of polyvinylidene fluoride membranes by UV light”, *React. Funct. Polym.*, **140**, 56-61.
<https://doi.org/10.1016/j.reactfunctpolym.2019.04.012>.
- Kamyar, S., Peter, F., Dianne, L. and Ranil, W.S. (2018), “Combined electrocoagulation and membrane distillation for treating high salinity produced waters”, *J. Membr. Sci.*, **564**, 82-96. <https://doi.org/10.1016/j.memsci.2018.06.041>.
- Kiss, A.A. and Kattan Read, O.M. (2018), “An industrial perspective on membrane distillation processes”, *J. Chem. Technol. Biot.*, **93**(8), 2047-2055.
<https://doi.org/10.1002/jctb.5674>.
- Kummu, M., Guillaume, J.H., De, M.H., Eisner, S., Flörke, M., Porkka, M., Siebert, S., Veldkamp, T.I. and Ward, P.J. (2016), “The world’s road to water scarcity: Shortage and stress in the 20th century and pathways towards sustainability”, *Sci. Rep.*, **6**(1), 38495. <https://doi.org/10.1038/srep38495>.
- Lai, C.Y., Groth, A., Gray, S. and Duke, M. (2014), “Enhanced abrasion resistant PVDF/nanoclay hollow fibre composite membranes for water treatment”, *J. Membr. Sci.*, **449**, 146-157.
<https://doi.org/10.1016/j.memsci.2013.07.062>.
- Li, H., Shi, W., Zeng, X., Huang, S., Zhang, H. and Qin, X. (2020), “Improved desalination properties of hydrophobic GO-incorporated PVDF electrospun nanofibrous composites for vacuum membrane distillation”, *Sep. Purif. Technol.*, **230**, 115889. <https://doi.org/10.1016/j.seppur.2019.115889>.
- Li, H., Zi, X., Shi, W., Qin, L., Zhang, H. and Qin, X. (2019), “Preparation of highly hydrophobic PVDF hollow fiber composite membrane with lotus leaf-like surface and its desalination properties”, *Membr. Water Treat.*, **10**(4), 287-298.
- Lin, J., Wu, X., Zheng, C., Zhang, P., Huang, B., Guo, N. and Jin, L. (2014), “Synthesis and properties of epoxy-polyurethane/silica nanocomposites by a novel sol method and in-situ solution polymerization route”, *Appl. Surf. Sci.*, **303**, 67-75.
<https://doi.org/10.1016/j.apsusc.2014.02.075>.
- Liu, C., Fang, Y., Miao, X., Pei, Y., Yan, Y., Xiao, W. and Wu, L. (2019), “Facile fabrication of superhydrophobic polyurethane sponge towards oil-water separation with exceptional flame-retardant performance”, *Sep. Purif. Technol.*, **229**, 115801. <https://doi.org/10.1016/j.seppur.2019.115801>.
- Liu, F., Zhu, B. and Xu, Y. (2006), “Improving the hydrophilicity of poly (vinylidene fluoride) porous membranes by electron beam initiated surface grafting of AA/SSS binary monomers”, *Appl. Surf. Sci.*, **253**(4), 2096-2101.
<https://doi.org/10.1016/j.apsusc.2006.04.007>.
- Liu, Q., Chen, D. and Kang, Z. (2015), “One-step electrodeposition process to fabricate corrosion resistant superhydrophobic surface on magnesium alloy”, *ACS Appl. Mater. Interf.*, **7**(3), 1859-67.
<https://doi.org/10.1021/am507586u>.

- Liu, T., Liu, Z., Li, N., Li, X., Wang, D., Huang, Q. and Xiao, C. (2017), "Superhydrophobicity and regeneration of PVDF/SiO₂ composite films", *Appl. Surf. Sci.*, **396**, 1443-1449. <https://doi.org/10.1016/j.apsusc.2016.11.184>.
- Liu, Y., Wang, J., Xiao, Z., Liu, L., Li, D., Li, X., Yin, H. and He, T. (2020), "Anisotropic performance of a superhydrophobic polyvinyl difluoride membrane with corrugated pattern in direct contact membrane distillation", *Desalination*, **481**, 114363. <https://doi.org/10.1016/j.desal.2020.114363>.
- Lu, X., Peng, Y., Ge, L., Lin, R., Zhu, Z. and Liu, S. (2016), "Amphiphobic PVDF composite membranes for anti-fouling direct contact membrane distillation", *J. Membr. Sci.*, **505**, 61-69. <https://doi.org/10.1016/j.memsci.2015.12.042>.
- Ma, W., Zhao, J., Oderinde, O., Han, J., Liu, Z., Gao, B., Xiong, R., Zhang, Q., Jiang, S. and Huang, C. (2018), "Durable superhydrophobic and superoleophilic electrospun nanofibrous membrane for oil-water emulsion separation", *J. Colloid Interf. Sci.*, **532**, 12-23. <https://doi.org/10.1016/j.jcis.2018.06.067>.
- Mcgaughey, A.L., Gustafson, R.D. and Childress, A.E. (2017), "Effect of long-term operation on membrane surface characteristics and performance in membrane distillation", *J. Membr. Sci.*, **543**, 143-150. <https://doi.org/10.1016/j.memsci.2017.08.040>.
- Meng, H., Wang, S., Xi, J., Tang, Z. and Jiang, L. (2008), "Facile means of preparing superamphiphobic surfaces on common engineering metals", *J. Phys. Chem. C*, **112**(30), 11454-11458. <https://doi.org/10.1021/jp803027w>.
- Naidu, G., Jeong, S. and Vigneswaran, S. (2014), "Influence of feed/permeate velocity on scaling development in a direct contact membrane distillation", *Sep. Purif. Technol.*, **125**, 291-300. <https://doi.org/10.1016/j.seppur.2014.01.049>.
- Nosonovsky, M. (2007), "On the range of applicability of the Wenzel and Cassie equations", *Langmuir*, **23**(19), 9919-9920. <https://doi.org/10.1021/la701324m>.
- Panagopoulos, A. and Haralambous, K.J. (2020), "Environmental impacts of desalination and brine treatment - Challenges and mitigation measures", *Mar Pollut Bull*, **161**, 111773. <https://doi.org/10.1016/j.marpolbul.2020.111773>.
- Panagopoulos, A., Haralambous, K.J. and Loizidou, M. (2019), "Desalination brine disposal methods and treatment technologies - A review", *Sci Total Environ*, **693**, 133545. <https://doi.org/10.1016/j.scitotenv.2019.07.351>.
- Qin, A., Wu, X., Ma, B., Zhao, X. and He, C. (2014), "Enhancing the antifouling property of poly (vinylidene fluoride)/SiO₂ hybrid membrane through TIPS method", *J. Mater. Sci.*, **49**(22), 7797-7808. <https://doi.org/10.1007/s10853-014-8490-y>.
- Rezaei, M., Warsinger, D.M., Lienhard, J.H.V., Duke, M.C., Matsuura, T. and Samhaber, W.M. (2018), "Wetting phenomena in membrane distillation: Mechanisms, reversal, and prevention", *Water Res.*, **139**, 329-352. <https://doi.org/10.1016/j.watres.2018.03.058>.
- Saifaldeen, Z.S., Khedir, K.R., Camci, M.T., Ucar, A., Suzer, S. and Karabacak, T. (2016), "The effect of polar end of long-chain fluorocarbon oligomers in promoting the superamphiphobic property over multi-scale rough Al alloy surfaces", *Appl. Surf. Sci.*, **379**, 55-65. <https://doi.org/10.1016/j.apsusc.2016.04.050>.
- Saleh, J.M., Ali, E.M., Orfi, J.A. and Najib, A.M. (2019), "Water cost analysis of different membrane distillation process configurations", *Membr. Water Treat.*, **11**(5), 363-374. <https://doi.org/10.12989/mwt.2020.11.5.363>.
- Tang, Y.P., Cai, T., Loh, D., O'Brien, G.S. and Chung, T.S. (2017), "Construction of antifouling lumen surface on a poly (vinylidene fluoride) hollow fiber membrane via a zwitterionic graft copolymerization strategy", *Sep. Purif. Technol.*, **176**, 294-305. <https://doi.org/10.1016/j.seppur.2016.12.012>.
- Vejayakumaran, P., Rahman, I.A., Sipaut, C.S., Ismail, J. and Chee, C.K. (2008), "Structural and thermal characterizations of silica nanoparticles grafted with pendant maleimide and epoxide groups", *J. Colloid Interf. Sci.*, **328**(1), 81-91. <https://doi.org/10.1016/j.jcis.2008.08.054>.
- Viswanadam, G. and Chase, G.G. (2012), "Contact angles of drops on curved superhydrophobic surfaces", *J. Colloid Interf. Sci.*, **367**(1), 472-477. <https://doi.org/10.1016/j.jcis.2011.11.004>.
- Wang, H., Fang, J., Cheng, T., Ding, J., Qu, L., Dai, L., Wang, X. and Lin, T. (2008), "One-step coating of fluoro-containing silica nanoparticles for universal generation of surface superhydrophobicity", *Chem. Commun.*, **7**, 877-879. <https://doi.org/10.1039/B714352D>.
- Wang, J.L. and Xu, L.J. (2012), "Advanced oxidation processes for wastewater treatment: formation of hydroxyl radical and application", *Crit. Rev. Env. Sci. Tec.*, **42**(3), 251-325. <https://doi.org/10.1080/10643389.2010.507698>.
- Wang, Y., He, G., Shao, Y., Zhang, D., Ruan, X., Xiao, W., Li, X., Wu, X. and Jiang, X. (2019), "Enhanced performance of superhydrophobic polypropylene membrane with modified antifouling surface for high salinity water treatment", *Sep. Purif. Technol.*, **214**, 11-20. <https://doi.org/10.1016/j.seppur.2018.02.011>.
- Wang, Z. and Lin, S. (2017), "Membrane fouling and wetting in membrane distillation and their mitigation by novel membranes with special wettability", *Water Res.*, **112**, 38-47. <https://doi.org/10.1016/j.watres.2017.01.022>.
- Wei, C., Dai, F., Lin, L., An, Z., He, Y., Chen, X., Chen, L. and Zhao, Y. (2018), "Simplified and robust adhesive-free superhydrophobic SiO₂-decorated PVDF membranes for efficient oil/water separation", *J. Membr. Sci.*, **555**, 220-228. <https://doi.org/10.1016/j.memsci.2018.03.058>.
- Xiao, Z., Zheng, R., Liu, Y., He, H., Yuan, X., Ji, Y., Li, D., Yin, H., Zhang, Y., Li, X. and He, T. (2019), "Slippery for scaling resistance in membrane distillation: A novel porous micropillared superhydrophobic surface", *Water Res.*, **155**, 152-161. <https://doi.org/10.1016/j.watres.2019.01.036>.
- Yu, L.Y., Xu, Z.L., Shen, H.M. and Yang, H. (2009), "Preparation and characterization of PVDF-SiO₂ composite hollow fiber UF membrane by sol-gel method", *J. Membr. Sci.*, **337**(1-2), 257-265. <https://doi.org/10.1016/j.memsci.2009.03.054>.
- Zhang, F., Shi, Z., Chen, L., Jiang, Y., Xu, C., Wu, Z., Wang, Y. and Peng, C. (2017), "Porous superhydrophobic and superoleophilic surfaces prepared by template assisted chemical vapor deposition", *Surf. Coat. Technol.*, **315**, 385-390. <https://doi.org/10.1016/j.surfcoat.2017.02.058>.
- Zhang, Y., Wang, X., Wang, C., Liu, J., Zhai, H., Liu, B., Zhao, X. and Fang, D. (2018), "Facile fabrication of zinc oxide coated superhydrophobic and superoleophilic meshes for efficient oil/water separation", *RSC Advances*, **8**(61), 35150-35156. <https://doi.org/10.1039/C8RA06059B>.
- Zhu, Z. and Dou, J. (2018), "Current status of reclaimed water in China: An overview", *J. Water Reuse Desal.*, **8**(3), 293-307. <https://doi.org/10.2166/wrd.2018.070>.